

Single-Shot Time-Domain Studies of Spin-Torque-Driven Switching in Magnetic Tunnel Junctions

Y.-T. Cui,¹ G. Finocchio,² C. Wang,¹ J. A. Katine,³ R. A. Buhrman,¹ and D. C. Ralph¹

¹Cornell University, Ithaca, New York 14853, USA

²Dipartimento di Fisica della Materia e Ingegneria Elettronica, University of Messina, Salita Sperone 31, 98166 Messina, Italy

³Hitachi Global Storage Technologies, San Jose, California 95135 USA

(Received 11 June 2009; published 1 March 2010)

We report single-shot measurements of resistance versus time for thermally assisted spin-torque switching in magnetic tunnel junctions. We achieve the sensitivity to resolve the magnetic dynamics prior to as well as during switching, yielding detailed views of switching modes and variations between events. Analyses of individual traces allow measurements of coherence times, nonequilibrium excitation spectra, and variations in magnetization precession amplitude. We find that with a small in-plane hard-axis magnetic field the switching dynamics are more spatially coherent than for a zero field.

DOI: 10.1103/PhysRevLett.104.097201

PACS numbers: 75.75.-c, 85.75.Dd

Magnetization switching induced by spin-transfer torque [1,2] is of interest both for probing the fundamental physics of magnetic dynamics and for applications in storage technologies [3]. Measurements in the time domain [4–10] can provide the most direct information about the dynamics. However, the majority of previous time-resolved studies of spin-torque switching [4–8] required averaging over many events, thereby hiding individual variations. Magnetic tunnel junctions (MTJs) can now provide resistance signals large enough for single-shot measurements, and initial experiments have measured resistance jumps associated with the completion of spin-torque switching in MTJs using single-shot techniques [9,10] but they could not resolve the smaller signals associated with the precessional dynamics that produce the switching. Here we demonstrate a technique for substantially improving the sensitivity of single-shot resistance measurements so that for the first time we observe directly the magnetic dynamics both prior to and during spin-torque switching. We obtain a view of the magnetic dynamics that is sufficiently detailed not only to assist in optimizing the switching process, but also to make MTJs promising model systems for probing the general properties of nonlinear systems subject to thermal fluctuations.

The MTJ samples that we study have the layer structure (in nm): bottom contact, synthetic antiferromagnet (SAF) pinned layer [IrMn(6.1)/CoFe(1.8)/Ru/CoFeB(2.0)], tunnel barrier [MgO], magnetic free layer [CoFe(0.5)/CoFeB(3.4)], top contact. Both the pinned and free layers are patterned into an elliptical $65 \times 130 \text{ nm}^2$ cross section parallel to the SAF pinning. All measurements are performed at room temperature, and positive current corresponds to electron flow from the free to the pinned layer. An easy axis hysteresis loop is shown in Fig. 1(a). Our discussion of current-driven reversal will focus on switching from the higher-resistance antiparallel (AP) state to the parallel (P) state but measurements of P-to-AP dynamics

are qualitatively similar. We will examine switching both in the case of zero total magnetic field on the free layer and in the case that a small (100 Oe) field is applied along the in-plane hard axis, to rotate the free layer approximately 15° from the AP configuration [see inset, Fig. 1(a)]. We will present data from one sample, but have studied two other devices in zero field and one other in the hard-axis field, with all showing the same differences depending on field geometry.

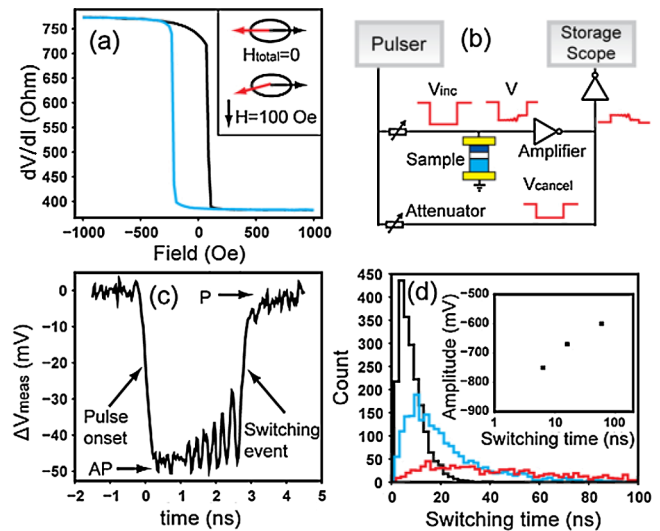


FIG. 1 (color online). (a) Resistance vs magnetic field applied along the easy axis. Inset: initial magnetization configurations for zero total field and for an 100 Oe in-plane hard-axis field for which the free layer rotates by $\sim 15^\circ$ relative to the stationary fixed layer. (b) Schematic of the measurement circuit. (c) An example of an AP-to-P switching trace for $V = -750 \text{ mV}$ and the 100 Oe hard-axis field. (d) Histograms of switching times for $V = -750 \text{ mV}$ (narrowest distribution), -670 mV , and -600 mV (broadest distribution). (inset) Pulse amplitude vs average switching time.

We perform single-shot measurements using the circuit shown in Fig. 1(b). After initializing the sample in the *AP* state we use a pulse generator to produce an 100 ns long, 300 ps rise-time negative pulse, split this signal with a power divider, and apply one part with amplitude V_{inc} to the sample through one rf probe. Using a second probe, we detect the transmitted pulse, $V(t) = V_{\text{inc}}/[1 + G_S(t)Z_0/2]$, where $G_S(t)$ is the sample conductance and $Z_0 = 50 \Omega$ is the probe impedance, and we amplify initially with one inverting amplifier with effective gain of 5 dB. A key step that substantially improves the dynamic range of the measurement is that we then combine the transmitted signal with the split-off copy of the original pulse using a time delay and attenuation tuned to cancel the part of the transmitted pulse that does not depend on the magnetic dynamics. This enables us to detect much smaller conductance changes than in previous single-shot measurements [9,10], because we can apply additional amplification without saturating the amplifiers before or during the pulse. We record the signal with an 11 GHz, 40 GSamples/s storage oscilloscope following a total net gain of 14 dB. When plotting *AP*-to-*P* switching events, we subtract an average baseline curve taken with the sample initialized to the *P* state, for which the negative pulse does not produce switching. Figure 1(c) shows a representative measurement $\Delta V_{\text{meas}}(t)$ for the 100 Oe hard-axis field and a transmitted pulse amplitude $V = -750$ mV. We achieve the sensitivity to observe conductance variations above the noise background throughout the period between the pulse onset and the switching event. The rms noise level corresponds to $\sim 2\%$ of the difference between *AP* and *P* conductances.

Before analyzing the time traces, we will first demonstrate that our data correspond to thermally-assisted spin-torque switching [11,12]. Figure 1(d) shows the switching-time distributions for three values of V , for the case of the 100 Oe hard-axis field. The broad widths of the distributions indicate that our pulse amplitudes $|V|$ are below the zero-temperature switching threshold so that switching is assisted by thermal fluctuations. The long-time tails of the distributions fit well to a simple exponential $\exp[-t/\tau_0(V)]$. Extrapolating the measured values of $\tau_0(V)$ [Fig. 1(d), inset] to 1 ns gives an estimate for the zero-temperature switching threshold of -870 mV. We have not attempted to investigate higher values of $|V|$ because the MTJs are not sufficiently stable.

Now we turn to the detailed dynamics revealed by the time traces. In Fig. 2(a) and 2(b), we show selected traces with different switching times for $V = -750$ mV, for both the 100 Oe hard-axis field and zero total field. We resolve the conductance oscillations prior to switching in both configurations, with oscillation amplitudes that fluctuate with time. In the right columns of Fig. 2(a) and 2(b) we zoom in to each trace 2 ns before and after switching. For the 100 Oe hard-axis field [Fig. 2(a)], most traces show at least a few cycles of large oscillations in the 2 ns

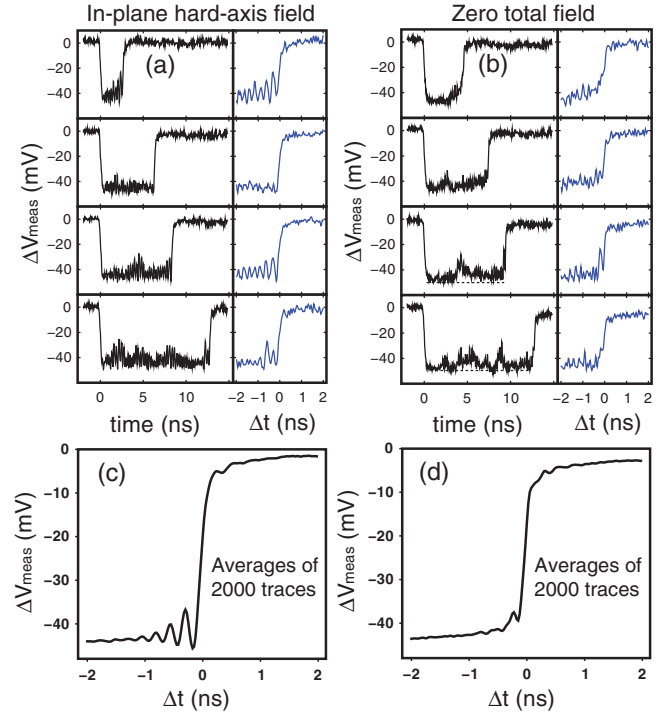


FIG. 2 (color online). Measured oscillatory signals leading up to switching for $V = -750$ mV. (a),(b) Representative switching traces for (a) an in-plane hard-axis field of 100 Oe and (b) zero total field, together with magnified views 2 ns before and 2 ns after the switching events. (c),(d) Average of 2000 measured traces with the switching edge aligned for (c) the in-plane hard-axis field and (d) zero total field.

prior to switching, corresponding to magnetic precession with large amplitude leading to reversal [1,3,5]. However, these oscillations show large variations from trace to trace, ranging from almost-vanishing amplitude (2nd curve in Fig. 2(a)) to oscillations close to half the difference between the initial ($\approx AP$) and final ($\approx P$) values. For the zero total field case, the conductance oscillations immediately prior to switching are much weaker [Fig. 2(b)]. Many traces for this case merely show a gradual increase in ΔV_{meas} without any significant oscillations immediately prior to switching.

Figures 2(c) and 2(d) show averages of 2000 traces with switching edges aligned, for the two field geometries. These averaged curves are very different from typical individual traces. Nevertheless, for the 100 Oe hard-axis field the averaged trace shows oscillations with increasing amplitude before switching [Fig. 2(c)], indicating that switching occurs preferentially at a particular phase of the conductance oscillations. The $(1/e)$ time scale for the averaged precession amplitude to build prior to reversal is 0.25 ± 0.02 ns for all V from -540 to -750 mV. This is likely a measure of the coherence time for dephasing between traces with differing precession angles, rather than a true measure of precession amplitude growth, because this scale is shorter than the correlation time for

amplitude changes (determined below). For the averaged trace in the case of zero total field [Fig. 2(d)], the oscillatory features are almost entirely washed out, suggesting much weaker correlations between the oscillation phase and the switching time.

We have performed micromagnetic simulations to understand these results, using the code described in [13,14]. The simulation parameters are: free-layer saturation magnetization $M_S = 1050$ emu/cm³, damping = 0.025, exchange = 1.3×10^{-11} J/m, uniaxial anisotropy = 4×10^3 J/m³, spin polarization = 0.6, and sample temperature = 400 K. The sample size is the same as in the experiment, the current density during the pulse is -2×10^7 A/cm², and the pinned layer is assumed to be immobile. We have implemented the simulations both with a spin-torque vector oriented strictly within the plane defined by the electrode magnetizations and also with an additional perpendicular component with magnitude 30% of the in-plane torque [15], and we found no qualitative differences in outcomes. All the simulation results we display will include the perpendicular torque. In Fig. 3, we plot examples of simulated conductance traces for the two field configurations discussed above and also

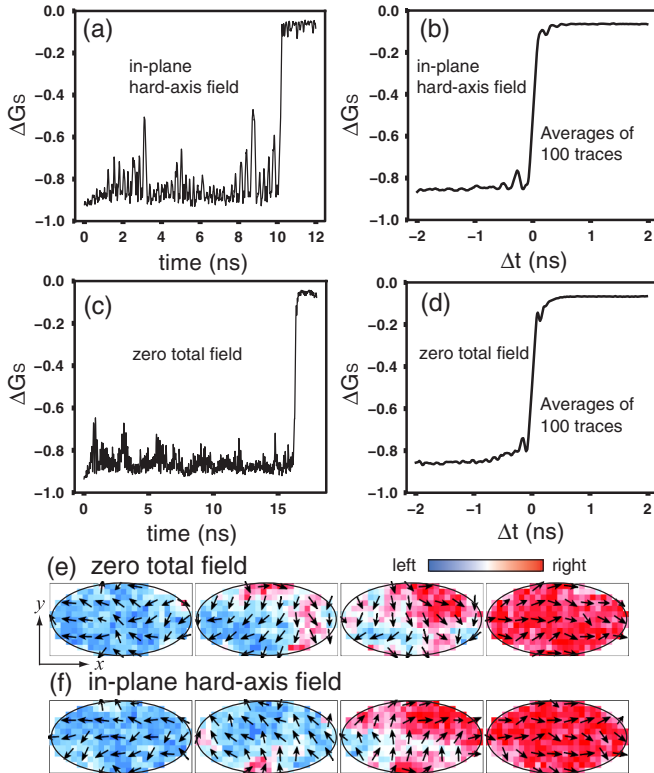


FIG. 3 (color online). (a),(c) Simulated switching traces for the two field geometries. The change in conductance is normalized by the difference $G_P - G_{AP}$. (b),(d) Averages of 100 simulated switching traces with the switching edges aligned. (e), (f) Snapshots with 70 ps spacing of micromagnetic configurations during the switching events. The color scale denotes the magnetization component along the x axis.

the averaged traces over 100 simulated reversals near the switching edges [compare to Figs. 2(c) and 2(d)]. The simulations reproduce many of the features seen in the experiment including the differences in the coherence of the oscillations between the two field geometries. The calculated magnetic configurations during switching events [Figs. 3(e) and 3(f)] suggest that the typical mechanism for reversal differs for the two field geometries. Switching for zero total field generally proceeds with one end of the sample switching first and the rest following by domain wall propagation [9] [Fig. 3(e)]. For the hard-axis field, the switching dynamics are generally more spatially uniform, albeit with local fluctuations [Fig. 3(f)]. Our measurements therefore support a prediction that a hard-axis field should promote macrospin switching behavior [16]. Our findings may also be related to observations that a large (~ 1000 Oe) hard-axis field decreases the linewidth of spin-torque nano-oscillators at large currents [17], although this is a very different dynamical regime.

The difference in the degree of spatial uniformity in our two field geometries can be observed directly in the time traces long before switching. For zero total field, the local minima in the fluctuations of $\Delta V_{\text{meas}}(t)$ exhibit excursions from the global minimum on scales of several ns, much longer than any precessional period [see especially the 3rd and 4th panels in Fig. 2(b)]. For the 100 Oe hard-axis field, the local minima in $\Delta V_{\text{meas}}(t)$ are more closely clustered near the AP value [Fig. 2(a)]. Large excursions of the sort present for the zero-field case are inconsistent with any approximately spatially-homogeneous dynamics for a thin-film magnetic sample, since at zero field the free-layer moment should pass close to the AP configuration twice per precessional cycle, each time giving the same global minimum in $\Delta V_{\text{meas}}(t)$.

The excellent sensitivity of our measurements allows us to analyze the magnetic dynamics even where the conductance oscillations are small, well away from the switching event. Figure 4(a) plots autocorrelation functions of the conductance versus time for the full interval between pulse onset and switching in the case of the 100 Oe hard-axis field, averaged over all switching traces with switching times longer than 10 ns at each value of V and normalized to the full difference between initial and final conductances. We find decoherence times Δt_c ranging from 0.54 ns at -540 mV to 0.45 ns at -750 mV [inset, Fig. 4(b)]. To help distinguish between frequency and amplitude variations, we plot in Fig. 4(b) autocorrelation functions of the oscillation amplitude versus peak number, determined by measuring every conductance peak between the pulse onset and switching. The coherence times for amplitude fluctuations Δt_A are greater than but comparable to Δt_c at each value of V , from which we conclude that both frequency and amplitude variations are significant in these \geq room temperature fluctuations. The corresponding coherence times predicted by our micromagnetic simulation

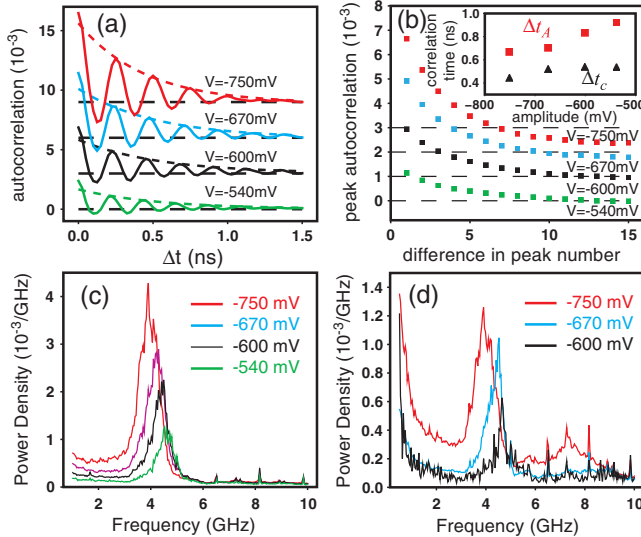


FIG. 4 (color online). (a) Autocorrelation functions of pre-switching conductance variations, normalized to the conductance difference before and after switching. The dotted lines are exponential fits to the peaks. The curves are offset vertically with horizontal lines denoting zero. (b) Autocorrelation functions for the conductance peak amplitude versus peak number. Inset: correlation times Δt_c from (a) and Δt_A from (b). Both (a) and (b) correspond to the 100 Oe in-plane hard-axis field configuration. (c) Averaged Fourier spectra of normalized conductance variations for the hard-axis field configuration. (d) Averaged Fourier spectra for zero total field.

are $\Delta t_c \approx \Delta t_A = 0.22 \pm 0.03$ ns, approximately independent of bias. In both the experiment and simulations, Δt_c and Δt_A are short, at most a few precession periods, showing that thermal fluctuations are a strong perturbation and simple pictures of zero-temperature dynamics [3] are not a good approximation. Surprisingly, the measured coherence times decrease with increasing values of $|V|$, whereas spin torque for $V < 0$ might be expected to decrease the effective damping and therefore increase the coherence time. We interpret the decrease in the coherence times with $|V|$ to be a sign of heating.

We can also Fourier transform our time traces for the pre-switching dynamics to achieve a measurement equivalent to thermally-excited ferromagnetic resonance [18], but accomplished for the very short-lived (< 100 ns) nonequilibrium state before switching. Figs. 4(c) and 4(d) show power spectra for the interval between the pulse onset and switching, averaged over all traces with switching times longer than 10 ns at each value of V for the two field geometries. For the 100 Oe hard-axis field [Fig. 4(c)], the spectra show a well-defined peak which with increasing $|V|$ grows in amplitude and shifts to lower frequency. The increasing amplitude of the peak can be explained by the reduction in effective magnetic damping due to the spin-

transfer torque [1,3], together with heating. The frequency shift can be understood as due primarily to the dependence of frequency on precession amplitude [19]. We estimate that the rms precession angle ranges from 8° for $V = -540$ mV to 14° for $V = -750$ mV for the 100 Oe hard-axis field. For zero total field [Fig. 4(d)], the Fourier spectra show weaker peaks, and possess a low-frequency tail. This is another indication of incoherent dynamics for this field geometry.

In summary, we have performed single-shot measurements of the resistance during thermally-assisted spin-torque-induced switching in MTJs, achieving for the first time the sensitivity to measure the magnetization dynamics both before and during individual switching events. Our technique provides measurements of coherence times and frequency spectra for the highly nonequilibrium, short-lived fluctuational dynamics preceding switching. The measurements also provide a detailed view that the switching mechanism can vary depending on the magnitude of a hard-axis magnetic field.

We thank P. Brouwer, B. Azzerboni, and L. Torres for discussions and D. Mauri for growing the MTJ layers. This work is supported by ONR, ARO, NSF (DMR-0605742), Spanish project MAT2008-04706/NAN, and NSF/NSEC through the Cornell Center for Nanoscale Systems. We also acknowledge NSF support through use of the Cornell Nanofabrication Facility/NNIN and the Cornell Center for Materials Research facilities.

- [1] J. C. Slonczewski, *J. Magn. Magn. Mater.* **159**, L1 (1996).
- [2] L. Berger, *Phys. Rev. B* **54**, 9353 (1996).
- [3] D. C. Ralph and M. D. Stiles, *J. Magn. Magn. Mater.* **320**, 1190 (2008).
- [4] R. H. Koch, J. A. Katine, and J. Z. Sun, *Phys. Rev. Lett.* **92**, 088302 (2004).
- [5] I. N. Krivorotov *et al.*, *Science* **307**, 228 (2005).
- [6] Y. Acremann *et al.*, *Phys. Rev. Lett.* **96**, 217202 (2006).
- [7] N. C. Emley *et al.*, *Phys. Rev. Lett.* **96**, 247204 (2006).
- [8] S. Serrano-Guisan *et al.*, *Phys. Rev. Lett.* **101**, 087201 (2008).
- [9] T. Devolder *et al.*, *Phys. Rev. Lett.* **100**, 057206 (2008).
- [10] H. Tomita *et al.*, *Appl. Phys. Express* **1**, 061303 (2008).
- [11] Z. Li and S. Zhang, *Phys. Rev. B* **69**, 134416 (2004).
- [12] D. M. Apalkov and P. B. Visscher, *Phys. Rev. B* **72**, 180405(R) (2005).
- [13] G. Finocchio *et al.*, *J. Appl. Phys.* **101**, 063914 (2007).
- [14] D. Aurelio, L. Torres, and G. Finocchio, *J. Magn. Magn. Mater.* **321**, 3913 (2009).
- [15] J. C. Sankey *et al.*, *Nature Phys.* **4**, 67 (2008).
- [16] K. Ito *et al.*, *J. Phys. D* **40**, 1261 (2007).
- [17] K. V. Thadani *et al.*, *Phys. Rev. B* **78**, 024409 (2008).
- [18] S. Petit *et al.*, *Phys. Rev. Lett.* **98**, 077203 (2007).
- [19] S. I. Kiselev *et al.*, *Nature (London)* **425**, 380 (2003).